

Temperature Dependence of Viscosity for Aqueous NaCl Solutions of Nonionic Rod-like Micelles in Dilute and Semidilute Regimes

TOYOKO IMAE,¹ MOTOI SASAKI, AND SHOICHI IKEDA

Department of Chemistry, Faculty of Science, Nagoya University, Nagoya 464, Japan

Received December 30, 1987; accepted March 30, 1988

The viscosity for aqueous micellar solutions of heptaoxyethylene alkyl ethers (C_nE_7 , $n = 12, 14, 16$) has been measured at different micelle and NaCl concentrations and at several temperatures under different shear rates. Rod-like micelles entangle one another above the threshold micelle concentration, $(c - c_0)^*$, which is higher than the threshold value of overlap, $(c - c_0)^*$, and decreases with a rise in temperature. The intrinsic viscosity at zero shear rate and at $(c - c_0)^*$ increases with the temperature, indicating the micellar growth. The relative viscosity at zero shear rate for aqueous NaCl solutions of entangled rod-like micelles in semidilute regime can be scaled against the micelle concentration, on the basis of the reptation model. The characteristic exponent, ν_r , increases as the temperature rises. This indicates the increase in rigidity or expansion of rod-like micelles. The complicated shear rate dependence on the relative viscosity is observed for micellar solutions above $(c - c_0)^*$, depending on the ν_r values of the rod-like micelles. The relation between the temperature dependence of viscosity and the liquid-liquid phase separation is discussed. © 1989 Academic Press, Inc.

INTRODUCTION

It is well known that aqueous solutions of oligooxyethylene alkyl ethers (C_nE_m) separate into two liquid phases above the lower critical solution temperature (LCST), and a number of workers have investigated the effect of temperature on the behavior of aqueous C_nE_m solutions within temperatures up to the lower consolute boundary.

While it was reported that C_nE_m micelles increased their sizes in water as the temperature rose (1–8), the critical concentration fluctuation or the change of the intermicellar interaction was suggested for scattering and diffusion experiments in the vicinity of the liquid-liquid phase separation (6–12).

The relation between the dehydration of surfactant molecules and the clouding phenomenon was described by Nilsson and Lindman (13).

The effect of temperature on the solution viscosity of C_nE_m micelles has been investigated by several workers. Elworthy and

McDonald (2) have reported that the intrinsic viscosity for aqueous solutions of $C_{16}E_7$, $C_{16}E_8$, and $C_{16}E_9$ have a certain threshold temperature, above which the intrinsic viscosity rises exponentially. Zulauf and Rosenbusch (10) have observed the gradual increase of the apparent intrinsic viscosity for C_8E_4 in water with the temperature and the sharp decrease of the viscosity above the lower consolute temperature. The increase of the apparent intrinsic viscosity with the temperature was also obtained for aqueous solutions of C_6E_3 , $C_{12}E_8$, $E_{14}E_7$ (11), and $C_{12}E_6$ (8).

We have investigated the liquid-liquid phase separation behavior of aqueous C_nE_7 solutions in the presence of NaCl (14). The lower consolute temperature decreased with an addition of NaCl. From the light scattering for aqueous NaCl solutions of C_nE_7 at 25°C, it was found that, if the alkyl chain is long or the added NaCl is concentrated, nonionic rod-like micelles are formed in a dilute regime and they overlap one another in a semidilute regime (15).

The analogy of light scattering and viscometric behaviors between elongated micelles

¹ To whom correspondence should be addressed.

and entangled polymer chains in semidilute solutions was discussed for cationic micelles, first, by Candau *et al.* (16, 17) and, later, by Imae *et al.* (18–21). The diffusion coefficient for aqueous solutions of $C_{12}E_5$ in semidilute regime was measured by Kato *et al.* (7).

In this work the relative viscosity for aqueous NaCl solutions of C_nE_7 ($n = 12, 14, 16$) is measured at different shear rates, NaCl and micelle concentrations, and temperatures, and the hydrodynamic behavior of nonionic rod-like micelles in dilute and semidilute solutions is discussed, referring to the liquid-liquid phase separation phenomenon.

EXPERIMENTAL

Monodisperse samples of C_nE_7 are the same as purchased from Nikko Chemicals Co., Ltd. (Tokyo) and previously used (14, 15). NaCl was ignited for 1 h and water was redistilled from alkaline $KMnO_4$.

The aqueous solutions of $C_{12}E_7$ in 4 M NaCl, $C_{14}E_7$ in 1 and 2 M NaCl, and $C_{16}E_7$ in 0 and 1 M NaCl were prepared at micelle concentrations of $(0.2-10) \times 10^{-2} \text{ g cm}^{-3}$. It was confirmed from light-scattering measurement (15) that rod-like micelles are dominantly formed in these solutions.

While a capillary viscometer of Ubbelohde type was used for measurements of low viscosity, a Haake Rotovisco RV12 concentric-cylinder rotational viscometer equipped with the coaxial double cylinder sensor system NV was used for viscous solutions. The temperature was changed from 15 to 45°C and the solutions were kept for 1 h at each temperature before measurement. The shear rates, G , were varied from 0.108 to 1385 s^{-1} . The details for the procedure using the rotational viscometer were described elsewhere (20).

The viscosity for viscous solutions was measured at several shear rates and was extrapolated in order to obtain the viscosity at zero shear rate, η^0 . The relative viscosity for micellar solutions at zero shear rate, $\eta_{\text{rel},\text{cmc}}^0$, is obtained by

$$\eta_{\text{rel},\text{cmc}}^0 = \eta^0 / \eta_{\text{cmc}} \approx \eta^0 / \eta_0 = \eta_{\text{rel}}^0, \quad [1]$$

where the viscosity at the critical micelle concentration, η_{cmc} , is identified with the viscosity of solvent, η_0 , since the critical micelle concentration is very low for all systems examined here. η_{rel}^0 is the relative viscosity for surfactant solutions at zero shear rate.

RESULTS

While dilute solutions display low viscosity and Newtonian flow which is independent of the shear rate, the high viscosity of solutions of high micelle concentrations changes with an increase in shear rate. Figure 1 illustrates the shear rate dependence of the relative viscosity for 1 M NaCl solutions of $C_{16}E_7$ at several micelle concentrations and temperatures. At 25°C, the relative viscosity decreases with an increase in shear rate, and the shear rate dependence is more drastic for solutions of higher micelle concentrations. Similar behavior is also observed for 1 M NaCl solutions of $C_{16}E_7$ at 20°C.

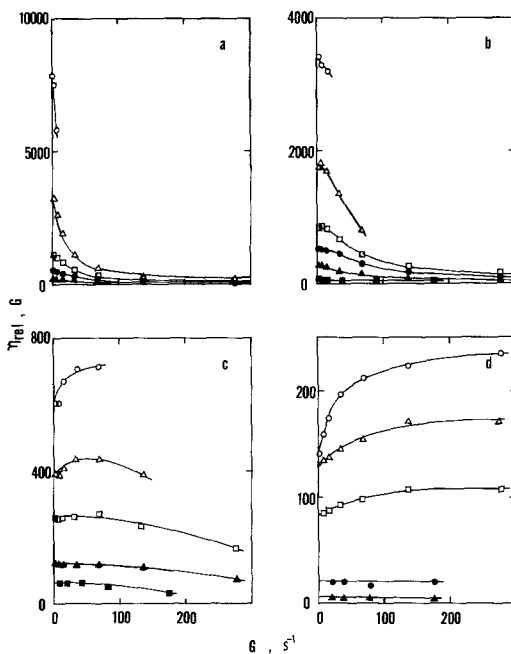


FIG. 1. The shear rate dependence of the relative viscosity for 1 M NaCl solutions of $C_{16}E_7$. Temperature (°C): a, 25; b, 30; c, 35; d, 40. Micelle concentration ($10^{-2} \text{ g cm}^{-3}$): ■, 2; ▲, 3; ●, 4; □, 5; △, 7; ○, 10.

At 30°C, the shear thinning of the relative viscosity becomes gradual and the relative viscosity seems to be constant at low shear rates for solutions of lower micelle concentrations. Similar curves are observed for solutions of low micelle concentrations at 35°C. However, at higher micelle concentrations above $5 \times 10^{-2} \text{ g cm}^{-3}$, the relative viscosity at 35°C increases at low shear rates and decreases through a maximum, as the shear rate increases. Such a shear thickening aspect with a maximum is revealed for solutions of micelle concentrations more than $4 \times 10^{-2} \text{ g cm}^{-3}$ at 40°C: the relative viscosity at 40°C still increases gradually, even if the shear rate is increased up to 277 s^{-1} .

The shear-rate dependence of the relative viscosity is also observed for aqueous solutions of C_{16}E_7 without NaCl: with temperatures of 20–45°C, while there is Newtonian flow for solutions of low micelle concentrations, the relative viscosity for solutions of high micelle concentrations displays shear-rate dependence with a flat part at low shear rates before shear thinning or with a maximum at a finite shear rate. The non-Newtonian flow for 1 and 2 M NaCl solutions of C_{14}E_7 and 4 M NaCl solutions of C_{12}E_7 is characterized by gradual shear

thinning with a flat part at low shear rates, and shear-rate dependence with a maximum or gradual shear thickening, but the variation is small.

Figure 2 shows the reduced viscosity at zero shear rate, $\eta_{sp}^0/(c - c_0) \equiv (\eta_{rel}^0 - 1)/(c - c_0)$, for 1 M NaCl solutions of C_{14}E_7 at several temperatures as a function of micelle concentration, $c - c_0$, where η_{sp}^0 represents the specific viscosity at zero shear rate. The inset illustrates the micelle concentration dependence of the reduced viscosity, $\eta_{sp}/(c - c_0)$, which was measured by the capillary viscometer.

While the reduced viscosity at 15°C increases almost linearly with micelle concentration, the reduced viscosity at 20°C deviates upward at high micelle concentrations from the initial slope. With an increase in temperature up to 35°C, the threshold micelle concentration for deviation decreases. At 40°C, the reduced viscosity increases gradually as micelle concentrations increase above the threshold value at $10^{-2} \text{ g cm}^{-3}$. This behavior is remarkable at 45°C: whereas the reduced viscosity at low micelle concentrations increases from 15 to 45°C, the situation is reversed for solutions of high micelle concentrations at 35, 40, and 45°C.

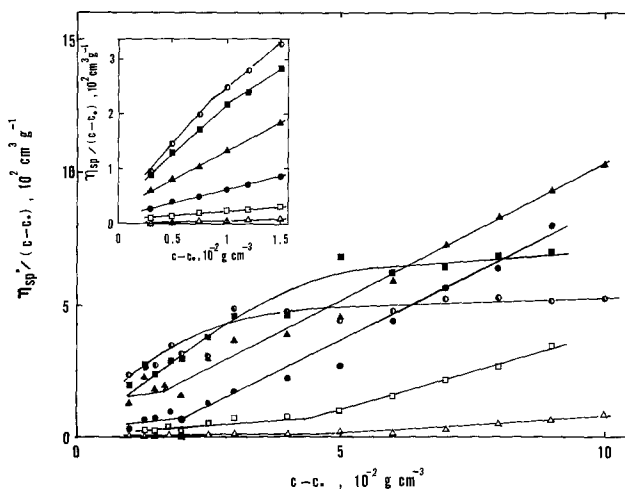


FIG. 2. The reduced viscosity at zero shear rate for 1 M NaCl solutions of C_{14}E_7 as a function of micelle concentration. Temperature (°C): Δ , 20; \square , 25; \bullet , 30; \blacktriangle , 35; \blacksquare , 40; \circ , 45. The inserted figure illustrates the reduced viscosity which was measured by a capillary viscometer.

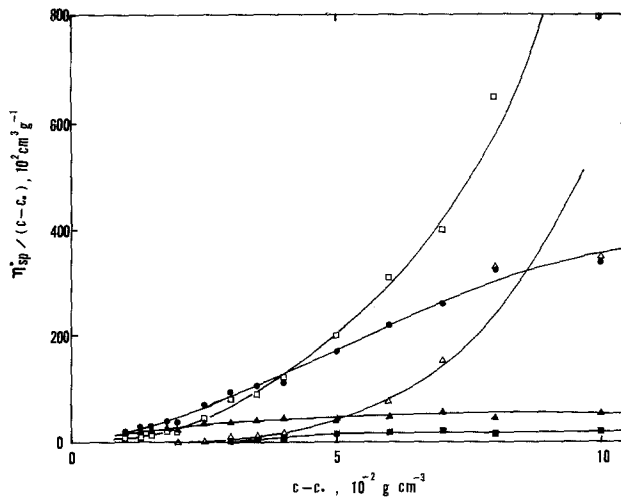


FIG. 3. The reduced viscosity at zero shear rate for 1 M NaCl solutions of C₁₆E₇ as a function of micelle concentration. The symbols represent the same temperature as in Fig. 2.

The reduced viscosity at zero shear rate for 1 M NaCl solutions of C₁₆E₇ is given in Fig. 3. The reduced viscosity at 20°C increases remarkably at high micelle concentrations but it is lower than that at 25°C. However, the reduced viscosity decreases at high micelle concentrations as the temperature rises from 25 to 40°C. A similar feature of the reduced viscosity against micelle concentrations and temperatures as seen in Figs. 2 and 3 was also obtained for C₁₂E₇ in 4 M NaCl, C₁₄E₇ in 2 M NaCl, and C₁₆E₇ in water.

The upward deviation of the reduced viscosity from the initial linear increase as observed for 1 M NaCl solutions of C₁₄E₇ at 20–35°C was observed for aqueous sodium halide solutions of alkyltrimethylammonium halides (20), and the threshold micelle concentration for deviation could be assigned to the threshold value of the entanglement of rod-like micelles, $(c - c_0)_\eta^*$.

The relative viscosity at zero shear rate for solutions of entangled rod-like micelles can be described by the relation

$$\eta_{rel}^0 \sim (c - c_0)^x \tag{2}$$

with

$$x = 3 / (3\nu_\eta - 1), \tag{3}$$

referring to

$$\eta_{rel}^0 \sim (m/m_\xi)^3, \tag{4}$$

analogous to the scaling laws for entangled polymer chains (22–24). m and m_ξ , respec-

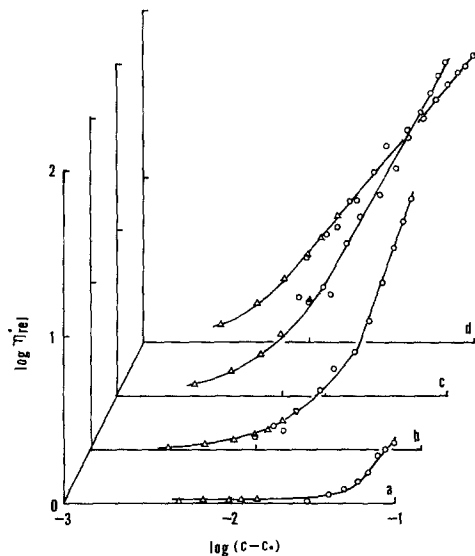


FIG. 4. The double logarithmic plot of the relative viscosity at zero shear rate vs micelle concentrations for 1 M NaCl solutions of C₁₄E₇. Temperature (°C): a, 15; b, 25; c, 35; d, 45. Data illustrated by triangle are the relative viscosity measured by a capillary viscometer.

tively, are aggregation number of rod-like micelles and aggregation number within the correlation length, ξ .

The relative viscosity at zero shear rate vs micelle concentration for 1 M NaCl solutions of $C_{14}E_7$ is plotted in a double logarithmic scale in Fig. 4. The relative viscosity measured by a capillary viscometer lies on the same line as the relative viscosity at zero shear rate or on its extension. In contrast with the gradual increase at low micelle concentrations, the logarithmic relative viscosity increases linearly against the logarithmic micelle concentration at high micelle concentrations. The micelle concentration, above which the linearity is realized, corresponds to the threshold value of entanglement, $(c - c_0)_\eta^*$. Table I lists the $(c - c_0)_\eta^*$ values for systems examined. The values are taken as micelle concentrations

where the reduced viscosity deviates from the initial straight line as in Fig. 2 or where the linearity of $\log \eta_{rel}^0$ vs $\log (c - c_0)$ starts as in Fig. 4. The values evaluated by two methods are consistent with each other and they also agree with the threshold value above which the non-Newtonian flow becomes remarkable, as demonstrated for aqueous sodium halide solutions of alkyltrimethylammonium halides (20).

Figure 5 gives the double logarithmic plot of the relative viscosity at zero shear rate against micelle concentrations above the threshold value of entanglement for aqueous NaCl solutions of C_nE_7 . The axis of the abscissa is arbitrarily shifted, and the shifted value is included in Table I. The linear relation is realized for all solutions, and the slope of the straight lines, the extensions of which

TABLE I
Viscometric Characteristics of Rod-like Micelles of C_nE_7 in Aqueous NaCl Solutions

	C_i (M)	T (°C)	$(c - c_0)_\eta^*$ (10^{-2} g cm $^{-3}$)	$[\eta]^*$ (10^2 cm 3 g $^{-1}$)	k'^*	$\log y$	x	ν_*
$C_{12}E_7$	4	15	2.9	0.29	0.369	0	1.66	0.94
		20	1-2	~0.63	0.370	0.32	1.24	1.14
		25	<1			0.49	1.07	1.27
$C_{14}E_7$	1	15	6.0	0.05	0.533			
		20	4.8	0.19	0.346	0.06	2.45	0.74
		25	4.3	0.46	0.374	0.22	2.91	0.68
		30	2.0	0.72	0.367	0.48	2.36	0.76
		35	1.7	1.05	0.373	0.70	1.89	0.86
		40	1.0	~1.40	0.357	0.90	1.49	1.00
		45	0.8	~1.45	0.357	1.06	1.23	1.15
	2	15	5.9	0.42	0.384	0	3.53	0.62
		20	3.5	0.93	0.387	0.32	2.65	0.71
		25	1-1.5	~1.45	0.384	0.62	2.09	0.81
30		<1			0.97	1.49	1.00	
$C_{16}E_7$	0	20	8.0	0.53	0.387	0	4.03	0.58
		25	3.5	0.90	0.388	0.32	3.85	0.59
		30				0.62	3.35	0.63
		35				0.85	2.76	0.70
		40				1.12	2.02	0.83
	1	20	3.8	~3.00	0.455	0	4.78	0.54
		25				0.46	3.18	0.65
		30				0.75	2.38	0.75
		35				1.15	1.42	1.04

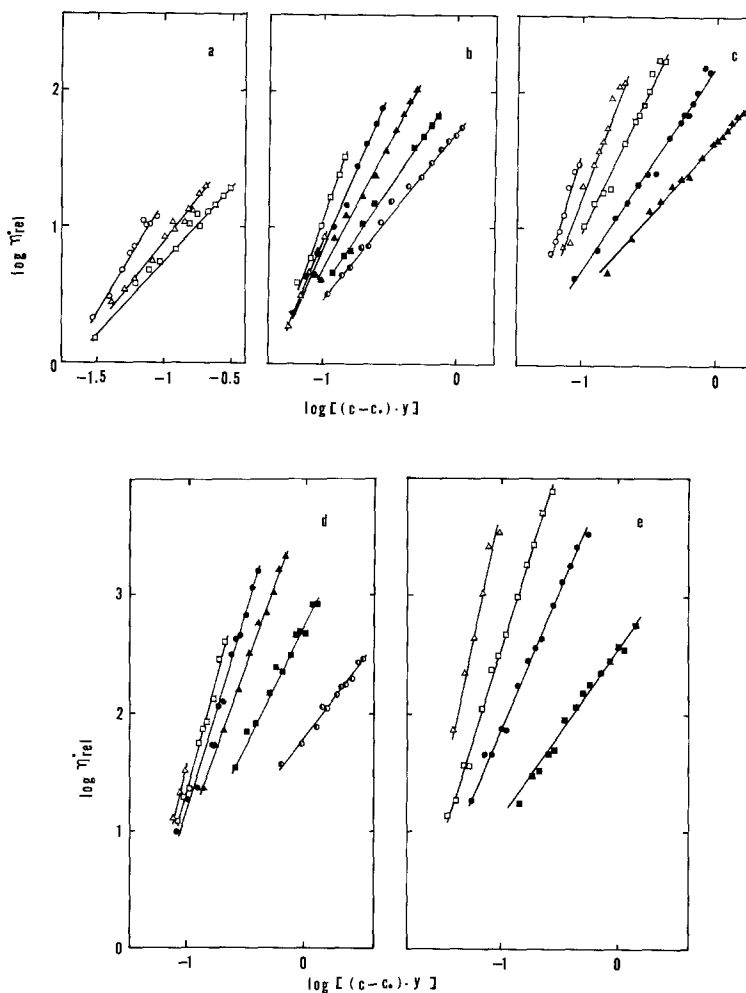


FIG. 5. The double logarithmic plot of the relative viscosity at zero shear rate vs micelle concentrations for aqueous NaCl solutions of C_nE_7 . a, $C_{12}E_7$ in 4 M NaCl; b, $C_{14}E_7$ in 1 M NaCl; c, $C_{14}E_7$ in 2 M NaCl; d, $C_{16}E_7$ in water; e, $C_{16}E_7$ in 1 M NaCl. The open circle, \circ , represents the temperature at 15°C and the other symbols represent the same temperature as in Fig. 2.

merge at a certain micelle concentration at a zero value of $\log \eta_{rel}^0$, gives the exponent, x , in Eq. [2]. The exponent, x , and the characteristic exponent, ν_η , are evaluated for each system and their values are listed in Table I.

For dilute micelle solutions, the relative viscosity is related to the micelle concentration by the Huggins equation,

$$\begin{aligned} (\eta_{rel}^0 - 1)/(c - c_0) &\equiv \eta_{sp}^0/(c - c_0) \\ &= [\eta] + k'[\eta]^2(c - c_0), \quad [5] \end{aligned}$$

or the Mead-Fuoss equation,

$$(\ln \eta_{rel}^0)/(c - c_0) = [\eta] - \beta[\eta]^2(c - c_0), \quad [6]$$

where $[\eta]$ represents the intrinsic viscosity at zero shear rate. k' and β are the hydrodynamic interaction coefficients and there is a relation such as

$$k' + \beta = \frac{1}{2} \quad [7]$$

between the two coefficients. Therefore, the relation

$$2(\eta_{sp}^0 - \ln \eta_{rel}^0)/(c - c_0)^2 = [\eta]^2 \quad [8]$$

is derived from Eqs. [5]–[7].

The intrinsic viscosity at each micelle concentration was calculated for solutions of micelle concentrations below $(c - c_0)_\eta^*$, on the basis of Eq. [8]. As seen in Fig. 6, the intrinsic viscosity for $C_{14}E_7$ micelles in 1 M NaCl increases with an increase in micelle concentration, indicating the micelle growth up to the threshold micelle concentration of entanglement. The increase of the intrinsic viscosity with micelle concentration was also observed for the other systems examined here. This behavior is in contrast to micelles of alkyltrimethylammonium halides in aqueous sodium halide solutions (20); the intrinsic viscosity of rod-like micelles of the alkyltrimethylammonium halides reached a constant value quickly at low micelle concentrations.

The values of the intrinsic viscosity at the threshold micelle concentration of entanglement, $[\eta]^*$, are listed for each system in Table I. By using the obtained value of the intrinsic viscosity, the Huggins constant was evaluated from Eq. [5]. The Huggins constant at the threshold micelle concentration of entanglement, k'^* , is between 0.35 and 0.39 for almost all systems, as seen in Table I. This value is of

the same magnitude as those for the alkyltrimethylammonium halides (20) and those for flexible polymer chains in good solvents (25).

DISCUSSION

The Threshold Micelle Concentration of Entanglement

The light scattering for aqueous NaCl solutions of C_nE_7 was measured and the characteristics of nonionic rod-like micelles were analyzed (15). The Debye plots and the diffusion coefficients at 25°C exhibit minimum values around the threshold micelle concentration of overlap, $(c - c_0)^*$, above which micelles overlap one another.

The threshold micelle concentration of overlap is defined by (26)

$$(c - c_0)^* \approx M/[(4\pi/3)R_G^3 N_A] \quad [9]$$

or

$$(c - c_0)^* = M/(R_G^3 N_A), \quad [9']$$

where M and R_G are the molecular weight and the radius of gyration, respectively, of rod-like micelles and N_A is Avogadro's number. The $(c - c_0)^*$ values for $C_{14}E_7$ in 1 and 2 M NaCl and $C_{16}E_7$ in water were evaluated as (0.57–1.08), (0.20–0.39), and (0.74–1.42) $\times 10^{-2}$

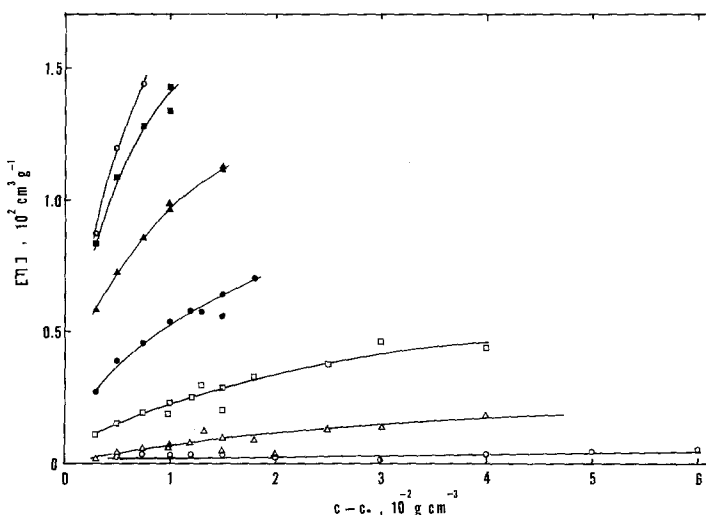


FIG. 6. The intrinsic viscosity for $C_{14}E_7$ micelles in 1 M NaCl. The symbols represent the same temperature as in Fig. 5.

g cm^{-3} , respectively, at 25°C from light-scattering experiments (15). These values are one-eighth to one-half times smaller than the $(c - c_0)_\eta^*$ values of 4.3, 1–1.5, and $3.5 \times 10^{-2} \text{ g cm}^{-3}$.

The discrepancy between $(c - c_0)^*$ and $(c - c_0)_\eta^*$ was also observed for aqueous sodium halide solutions of alkyltrimethylammonium halides (20). This behavior means that the entanglement of rod-like micelles takes place at a higher micelle concentration than for overlap. It may be inferred that there are four distinct regions: dilute, semidilute but nonentangled, semidilute and entangled, and concentrated. The existence of these regions was provided for polystyrene and polybutadiene in a good solvent (27).

The threshold micelle concentration of entanglement at each temperature for aqueous NaCl solutions of C_nE_7 is plotted in Fig. 7. The threshold value of entanglement decreases with increasing temperature, NaCl concentration, and alkyl chain length, consistent with the tendency of micelle growth, and suggesting the effect of the aggregation number of rod-like micelles on the threshold value of entanglement.

The Viscosity of Dilute Solutions

The viscosity for aqueous NaCl solutions of C_nE_7 at micelle concentrations below the threshold value of entanglement increases with rising temperature, as seen in Figs. 2 and 4. The intrinsic viscosity for aqueous NaCl solutions of C_nE_7 at the threshold micelle concentration of entanglement is plotted in Fig. 8 as a function of temperature. The $[\eta]^*$ value increases with an increase in temperature, NaCl concentration, and alkyl chain length, indicating the micelle growth. This behavior of temperature dependence is the same as that already reported on the intrinsic viscosity at infinite dilution and the apparent intrinsic viscosity at finite micelle concentration for aqueous solutions of C_nE_m (2, 8, 10, 11).

Elworthy and McDonald (2) found the temperature of 22°C as the threshold value of

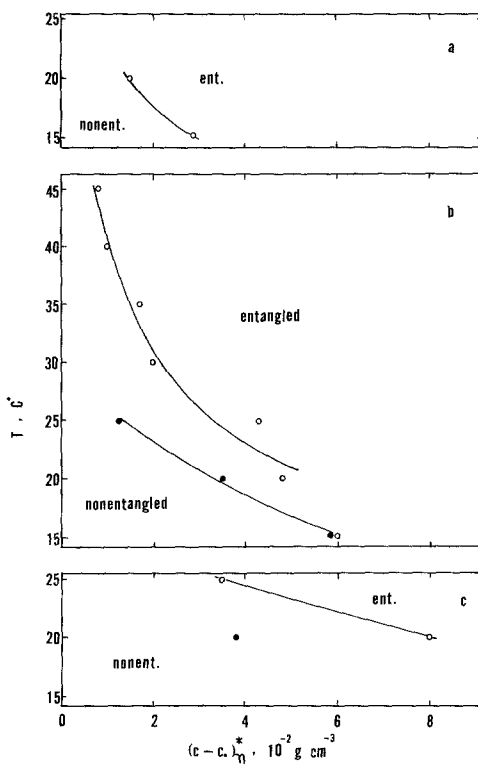


FIG. 7. The relation between the threshold micelle concentration of entanglement and the temperature for aqueous NaCl solutions of C_nE_7 . a, $C_{12}E_7$: \circ , 4 M NaCl. b, $C_{14}E_7$: \circ , 1 M NaCl; \bullet , 2 M NaCl. c, $C_{16}E_7$: \circ , water; \bullet , 1 M NaCl.

the sphere–rod transition on the intrinsic viscosity of aqueous solutions of $C_{16}E_7$. Such a threshold temperature was not observed on the $[\eta]^*$ value for aqueous NaCl solutions of C_nE_7 in the present work, since the addition of NaCl should lower such a threshold temperature.

Entangled Rod-like Micelles

For linear polymers in semidilute solutions, the reptation model (22, 23) is presented. If the reptation model is applied to entangled rod-like micelles in semidilute solutions, the relative viscosity at zero shear rate is scaled against the micelle concentration as in Eq. [2]. The x values in Eq. [2] are plotted in Fig. 9 as a function of temperature. The x values for nonionic micelles of C_nE_7 , except those for

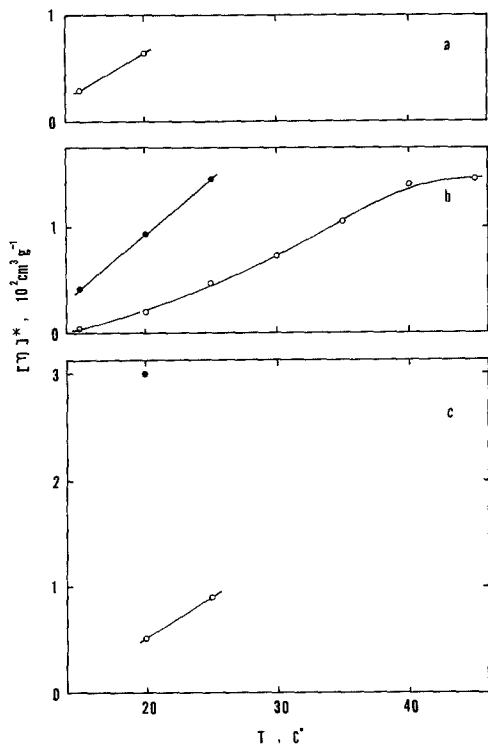


FIG. 8. The intrinsic viscosity at the threshold micelle concentration of entanglement for aqueous NaCl solutions of C_nE_7 as a function of temperature. The symbols have the same meanings as in Fig. 7.

$C_{14}E_7$ in 1 M NaCl and $C_{16}E_7$ in water at 20°C, decrease remarkably with an increase in temperature and slightly with an increase in NaCl concentration. Incidentally, the x values at 25°C for micelles of the alkyltrimethylammonium halides in aqueous sodium halide solutions were less dependent on salt concentration and alkyl chain length and ranged between 2.2–3.0 (20).

As seen in Table I, the ν_η values for rod-like micelles of C_nE_7 in aqueous NaCl solutions increase, depending on an increase of temperature and NaCl concentration. Roughly speaking, the ν_η values may be regarded as a measure of the rigidity or expansion of rod-like micelles (20). Then, as the temperature rises, a decrease of the flexibility or an increase of the rigidity or expansion is suggested for rod-like micelles of C_nE_7 .

Shear Rate Dependence of the Viscosity

While the viscosity of dilute micellar solutions of C_nE_7 is Newtonian flow, the viscosity of aqueous C_nE_7 solutions at high micelle concentrations changes complexly with the shear rate: for 1 M NaCl solutions of $C_{16}E_7$ at 20 and 25°C, the relative viscosity decreases with an increase in shear rate. For 1 M NaCl solutions of $C_{16}E_7$ at higher temperatures, for aqueous solutions of $C_{16}E_7$ without NaCl, for 1 and 2 M NaCl solutions of $C_{14}E_7$, and for 4 M NaCl solutions of $C_{12}E_7$, the relative viscosity shows a flat part at low shear rates before shear thinning, a maximum at a finite shear rate, or a gradual shear thickening, if the micelle concentration is high.

It can be generalized that the shear thinning is observed for solutions of rod-like micelles with smaller ν_η values and that the shear thickening occurs in solutions of rod-like micelles with larger ν_η values. Therefore, it is concluded

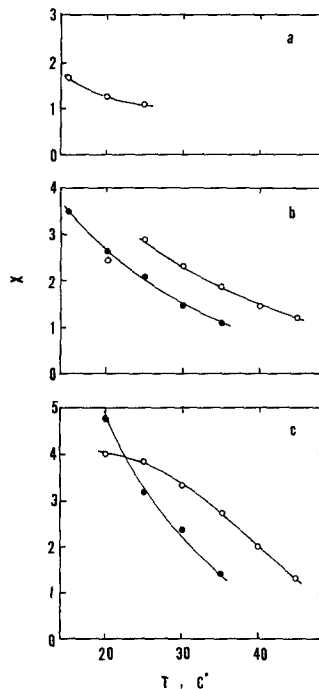


FIG. 9. The relation between the exponent, x , and the temperature for aqueous NaCl solutions of C_nE_7 . The symbols have the same meanings as in Fig. 7.

that, if rod-like micelles are more flexible, the entangled rod-like micelles are aligned or destroyed easily by the application of shear forces. On the other hand, in semidilute solutions of more rigid or expanded rod-like micelles, micelles suffer no effect or tighten further at low shear rates and then are aligned or destroyed at high shear rates.

Pseudoplastic behavior where the relative viscosity decreases with shear rate was observed for aqueous sodium halide solutions of the alkyltrimethylammonium halides (20). In the same work, it was demonstrated that the threshold micelle concentration of entanglement was consistent with the threshold micelle concentration above which the solutions become non-Newtonian.

Hoffmann *et al.* (28) have reported the shear rate dependence of the viscosity of some aqueous surfactant solutions. The viscosity for aqueous NaBr solutions of tetradecylpyridinium salicylate and its mixture with tetradecyltrimethylammonium salicylate exhibited the shear thinning behavior. On the other hand, the viscosity of aqueous solutions of tetradecyltrimethylammonium salicylate changed complexly with an increase in shear rate (29): the viscosity maintained constant at low shear rates, increased above a certain shear rate, and then decreased at higher shear rates. They suggested the possibility of a shear-induced phase transition, in which the micelle structure underwent the flow induced sol-gel transition.

CONCLUSION

We have measured the viscosity for aqueous NaCl solutions of C_nE_7 at different micelle and NaCl concentrations under the shear rate and have investigated its temperature dependence. Some conclusions were obtained: with an increase in temperature up to the lower consolute boundary, the intrinsic viscosity of rod-like micelles increases; that is, rod-like micelles grow in length but, simultaneously, micelles lose their flexibility. The threshold micelle concentrations for entanglement of rod-like micelles shift to lower micelle concentrations

at higher temperatures. The addition of NaCl and the increase of alkyl chain length have the same effect as temperature. While the viscosity behavior of solutions of more flexible rod-like micelles is pseudoplastic or shear thinning, solutions of more rigid or expanded rod-like micelles are subject to slight shear thickening and some of the solutions exhibit shear thinning at higher shear rates.

The relations of the micelle growth and the intermicellar interaction with the liquid-liquid phase separation were discussed by several workers. While it was suggested that nonionic C_nE_m micelles grew in water with a rise in temperature (1-8), it was pointed out that the increase of scattering intensity and apparent hydrodynamic radius accompanying the increase in temperature in the vicinity of the lower boundary for phase separation was not due to the micelle growth but originated in the critical concentration fluctuation resulting from the change of the intermicellar interaction with the elevation of temperature (9,10,12).

Corti *et al.* (11) have indicated that the miscibility in water of oligooxyethylene alkyl ethers with short alkyl chains is dominated by the interaction among small globular micelles and that the miscibility of surfactants with long alkyl chains is affected by the micellar growth besides the intermicellar interaction.

We have recently suggested that the liquid-liquid phase separation with the lower consolute temperature is induced by the destruction of the micelle-water interaction by the dehydration and the strengthening of the micelle-micelle attractive interaction by the micelle growth (14).

In this work, we obtained the result that the intrinsic viscosity for aqueous NaCl solutions of C_nE_7 micelles increases with an increase in temperature, indicating the micelle growth. However, the increase of the intrinsic viscosity is perceived at dilute micelle concentrations, and almost all of the solutions in the vicinity of the lower consolute boundary belong to a semidilute regime, as seen in Fig. 7. Moreover, the influence of the critical concentration

fluctuation on the viscosity behavior is not detectable.

Water hydrating C_nE_7 micelles may be dehydrated with a rise in temperature. The dehydration acts to weaken the micelle-water interaction. Rod-like C_nE_7 micelles become longer and entangle each other with increasing temperature. Therefore, the micelle-micelle attractive interaction grows stronger. These two effects can induce the liquid-liquid phase separation of aqueous C_nE_7 solutions at high temperature.

However, it was shown that there was no direct relation between surfactant dehydration and the clouding phenomenon (13). Moreover, it was stated that the increase of scattering intensity or apparent hydrodynamic radius was not due to the micelle growth, as described above. Therefore, the liquid-liquid phase separation behavior of aqueous surfactant solutions should be the subject of further discussion.

REFERENCES

- Balmбра, R. R., Clunie, J. S., Corkill, J. M., and Goodman, J. F., *Trans. Faraday Soc.* **58**, 1661 (1962); **60**, 979 (1964).
- Elworthy, P. H., and McDonald, C., *Kolloid Z. Z. Polym.* **195**, 16 (1964).
- Fujimatsu, H., Takagi, K., Matsuda, H., and Kuroiwa, S., *J. Colloid Interface Sci.* **94**, 237 (1983).
- Nilsson, P.-G., Wennerström, H., and Lindman, B., *J. Phys. Chem.* **87**, 1377 (1983).
- Zana, R., and Weill, C., *J. Phys. Lett.* **46**, L-953 (1985).
- Kato, T., and Seimiya, T., *J. Phys. Chem.* **90**, 3159 (1986).
- Kato, T., Anzai, S., and Seimiya, T., *J. Phys. Chem.* **91**, 4655 (1987).
- Wilcoxon, J. P., and Kaler, E. W., *J. Chem. Phys.* **86**, 4684 (1987).
- Hayter, J. B., and Zulauf, M., *Colloid Polym. Sci.* **260**, 1023 (1982).
- Zulauf, M., and Rosenbusch, J. P., *J. Phys. Chem.* **87**, 856 (1983).
- Corti, M., Minero, C., and Degiorgio, V., *J. Phys. Chem.* **88**, 309 (1984).
- Zulauf, M., Weckström, K., Hayter, J. B., Degiorgio, V., and Corti, M., *J. Phys. Chem.* **89**, 3411 (1985).
- Nilsson, P.-G., and Lindman, B., *J. Phys. Chem.* **87**, 4756 (1983).
- Imae, T., Sasaki, M., Abe, A., and Ikeda, S., *Langmuir* **4**, 414 (1988).
- Imae, T., *J. Phys. Chem.* (1988), in press.
- Candau, S. J., Hirsch, E., and Zana, R., *J. Phys. (Paris)* **45**, 1263 (1984).
- Candau, S. J., Hirsch, E., and Zana, R., *J. Colloid Interface Sci.* **105**, 521 (1985).
- Imae, T., and Ikeda, S., *J. Phys. Chem.* **90**, 5216 (1986).
- Imae, T., and Ikeda, S., *Colloid Polym. Sci.* **265**, 1090 (1987).
- Imae, T., Abe, A., and Ikeda, S., *J. Phys. Chem.* **92**, 1548 (1988).
- Sasaki, M., Imae, T., and Ikeda, S., *Langmuir* (1989), in press.
- de Gennes, P. G., *Macromolecules* **9**, 594 (1976).
- de Gennes, P. G., "Scaling Concepts in Polymer Physics." Cornell Univ. Press, Ithaca/New York/London, 1979.
- Doi, M., *J. Polym. Sci., Polym. Lett. Ed.* **19**, 265 (1981).
- Tanford, C., "Physical Chemistry of Macromolecules." Wiley, New York/London, 1961.
- Ying, Q., and Chu, B., *Macromolecules* **20**, 362 (1987).
- Graessley, W. W., *Polymer* **21**, 258 (1980).
- Hoffmann, H., Löbl, H., Rehage, H., and Wunderlich, I., *Tenside Deterg.* **22**, 6 (1985).
- Rehage, H., Wunderlich, I., and Hoffmann, H., *Prog. Coll. Polym. Sci.* **72**, 51 (1986).